© 2011 Wiley Periodicals, Inc.

Original Article

Embryo Developmental Disruption During Organogenesis Produced by CF-1 Murine Periconceptional Alcohol Consumption

Tamara A. Coll,[1] Leticia Perez Tito,[1] Cristian M.A. Sobarzo,[2] and Elisa Cebral[1]*

[1]Laboratorio de Reproducción y Fisiopatología Materno-Embrionaria, Instituto de Fisiología, Biología Molecular y Neurociencias (IFIBYNE-CONICET), Departamento de Biodiversidad y Biología Experimental (DBBE), Facultad de Ciencias Exactas y Naturales (FCEyN), Universidad de Buenos Aires (UBA), Buenos Aires, Argentina
[2]Instituto de Investigaciones en Reproducción, Facultad de Medicina, Universidad de Buenos Aires, Buenos Aires, Argentina

The aim was to study the control females (CF)-1 mouse embryo differentiation, growth, morphology on embryonic E- and N-cadherin expression at midgestation after periconceptional moderate alcohol ingestion. Adult female mice were exposed to 10% ethanol in drinking water for 17 days previous to and up to day 10 of gestation (ethanol-exposed females, EF) and were compared with nonexposed CF. EF presented reduced quantities of E10 to E10.5 embryos, greater percentage of embryos at stages less than E7.5, reduced implantation site numbers/female, and increased resorptions compared with CF. EF-embryo growth was significantly affected as evidenced by reduced cephalic and body sizes of E10 and E10.5 embryos (scanning electron microscopy) and decreased protein content of E10.5 embryos vs. CF embryos. A significantly higher percentage of EF-E10-10.5 embryos presented abnormal neural tube (NT) closure vs. the percentage of CF. E10 embryos from EF presented elevated tissue disorganization, pyknosis and nuclear condensation in somites, mesenchymal and neuroepithelial tissue. Immunohistochemical E- and N-cadherin distribution patterns were similar in organic structures of E10 embryos between groups. However, western blot revealed that E- and N-cadherin expression levels were significantly increased in EF-derived embryos vs. controls. Perigestational ethanol consumption by CF-1 mice induced significant damage in the organogenic embryogenesis by producing delayed differentiation, growth deficiencies, and increasing the frequency of NT defects. Ethanol exposure may disrupt cell–cell adhesion leading to upregulation of E- and N-cadherin expression suggesting that deregulation of cell adhesion molecules could be involved in the disruption of embryo development at organogenesis in CF-1 mouse. *Birth Defects Res (Part B)* 92:560–574, 2011. © 2011 Wiley Periodicals, Inc.

Key words: ***organogenesis; differentiation; growth; morphology; cadherins; alcohol; CF-1 mouse***

INTRODUCTION

It is well established that ethanol consumption by the mother disrupts fetal development in humans and in several species of experimental animals and constitutes an important medical issue with public and social complications (Ceccanti et al., 2007; Mancinelli et al., 2007; Aragón et al., 2008). Prenatal ethanol defects manifested in infants born with *Fetal Alcohol Spectrum Disorders* (FASD) (Hanningan and Armant, 2000) have been linked to craniofacial dysmorphogenesis, abnormal limb development, microencephaly, low birth weight, and mental and motor control deficiencies (Sampson et al., 2000; Hoyme et al., 2005; Mattson and Riley, 2008). It is well established that teratogenic effects of maternal ethanol exposure are dependent on several important variables. A critical gestational period during which ethanol induces craniofacial defects occurs during the third and fourth weeks postfertilization (gastrulation and organogenesis) in humans, a developmental period when neural tube (NT) formation progresses (Cook et al., 1987).

At present, little is known about susceptibility of outbred mouse strains to gestational alcohol exposure (Crabbe et al., 1994). Control females (CF)-1 embryo and fetal developmental response to prolonged ethanol ingestion was partially investigated by Soltes et al.

*Correspondence to: Elisa Cebral, LARFIMAE-CONICET, Intendente Güiraldes 2620, Ciudad Universitaria, Pabellón 2, 4to. Piso, Lab 22. (CP: 1428EGA). Ciudad Autónoma de Buenos Aires, Argentina.
E-mail: ecebral@hotmail.com
Received 30 April 2011; Accepted 11 July 2011

Grant sponsor: PLACIRH; Grant number: PRE-037/2000; Grant sponsor: Consejo Nacional de Investigaciones Científicas y Técnicas (CONICET); Grant number: PIP-CONICET: 5917|114-200801-00014; Grant sponsor: National Agency; Grant number: BID-PICT-2008-2210; Grant sponsor: UBACYT; Grant number: 20020090200655.

Published online in Wiley Online Library (wileyonlinelibrary.com)
DOI: 10.1002/bdrb.20329

(1996) and our group (Cebral et al., 2007). However, embryo dysmorphogenesis at organogenesis after moderate alcohol exposure by oral administration before gestation and during early pregnancy in CF-1 strain remained to be clarified.

The mechanisms by which ethanol produces FASD are not fully understood and are still subject to debate (Goodlett and Horn, 2001; Guerri, 2002). However, a number of different animal models and ethanol administration paradigms have been developed to investigate the mechanisms by which ethanol produces adverse effects (Dunty et al., 2002; Allan et al., 2003; Cudd, 2005; Rhodes et al., 2007; Boehm et al., 2009). One of the precise causes of disturbed embryonic development due to maternal ethanol consumption may be alterations of cell adhesion, in which cadherins play important roles. Cadherins are a family of dynamic transmembrane multiglycoproteins involved in proliferation, dissociation–reaggregation, migration, cell fate, neurite outgrowth, synaptogenesis, cell polarity, cell migration, and aggregation (Montell, 1999; Tepass et al., 2000), establishing an intimate relationship between junction formation and cell polarity (Nelson, 2003). Cadherins mediate calcium-dependent cell-to-cell adhesion in solid tissues and are critical for determining and maintaining the differentiation and architecture of epithelial tissues (Takeichi, 1991). The classic cadherin subfamily comprises well-characterized E-, N-, and P-cadherins that interact intracellularly with β-catenins and $p120^{ctn}$ (p120 catenin; Gumbiner, 2000). Cadherin isoforms have been identified in a tissue-specific manner and were shown to regulate morphogenesis through homophilic binding (Nose et al., 1988; Takeichi, 1990). E- and N-cadherin are important during embryogenesis where their expression patterns change spatiotemporally, whereas their switch has a marked impact on mechanical adhesion of cells (Wheelock et al., 2008). Altered expression of E-cadherin is involved in epithelial to mesenchymal transition and acquisition of a migrating phenotype (Savagner, 2001). Consequently, loss of E-cadherin is considered a driving force for epithelial cells to convert to mesenchymal cells during mesoderm formation. N-cadherin, the neural cell adhesion molecule, has roles in neuronal differentiation (Gao et al., 2001), synaptogenesis, modulation of dendrite spine shapes (Goda, 2002), neuronal survival, synaptic plasticity (Susuki et al., 2004), and somitogenesis (Radice et al., 1997).

At present, to the best of our knowledge, no study reported effects of perigestational ethanol exposure on early organogenic embryo cadherin expression. Altered cadherins could be particularly attractive mechanisms to explain some neurodevelopmental and growth abnormalities induced by maternal alcohol exposure.

The morphogenic susceptibility of CF-1 embryo to a moderate concentration of ethanol intake before gestation and up to organogenesis has not been studied. If adverse effects after ethanol exposure can be established in this outbred mouse strain, some important mechanisms of alcohol-induced teratogenesis could be elucidated with confidence. The aim of this work was to ascertain effects of oral ethanol perigestational exposure on CF-1 embryo differentiation, growth, and morphology in the organogenic period. We also addressed defects on embryonic cadherins in order to evaluate a possible relation to embryo dysmorphogenesis after moderate periconceptional alcohol ingestion.

MATERIALS AND METHODS

Animal Model

Outbred CF-1 sexually mature mice (*Mus musculus*) from the colony of the Facultad de Ciencias Exactas y Naturales (FCEyN) [School of Exact and Natural Sciences] of the University of Buenos Aires, (Buenos Aires, Argentina) were housed in groups of three to five mice in separate same-sex communal cages and kept in controlled room temperature (22°C) and light cycle (14 hr light: 10 hr dark). They were fed commercial mouse chow (Alimento ''Balanceado Cooperación Rata-Ratón,'' from the ''Asociación Cooperativa de Alimentos,'' S.A. Buenos Aires, Argentina) ad libitum and tap water. Sterile wood shavings were used as bedding and the air in habitats was renewed eight times a day. CF-1 female mice were 60 days old, and average body weight was between 27 and 30 g at the outset of ethanol treatment.

Experimental Ethanol Exposure

Experiments were carried out in accordance with the guidelines of the National Institute of Health and the FCEyN (Res CD 140/00) for the Care and Use of Laboratory Animals.

Adult female mice were orally exposed to 10% (w/v) ethanol in drinking water ad libitum for a total of 27 days, and the ethanol solution was replaced every 2 days. In each CF-1 female, the estrous cycle was evaluated daily throughout the first 15 days of 10% ethanol treatment, previous to fertilization. Since we observed that ethanol ingestion produced anestrous and continuous diestrum beginning on day 7 of ethanol exposure in about 80% of CF-1-treated females, on day 15 of ethanol administration females were superovulated. They were intraperitoneally injected with 5 IU of Pregnant Mare's Serum Gonadotropin (PMSG; Sigma Chemical Company, St Louis, MO) at 13:00 hr, and 48 hr later (on day 17 of ethanol treatment) 5 IU of Human Chorionic Gonadotrophin (hCG; Sigma Chemical Company) was applied. At the moment of hCG injection, one CF-1 female was placed with a mature fertile CF-1 male. The next day morning, mating was confirmed by observation of vaginal plug (day 1 of gestation) and CF-1-mated females were housed again with administration of 10% ethanol up to day 10 of gestation. CF received ethanol-free drinking water ad libitum and were superovulated with 5 IU/female PMSG/hCG, mated and allowed to continue gestation up to day 10. Pregnant control (C) and ethanol-treated female mice (T) were weighed at the beginning, throughout and at the end of treatment to record changes in body weight. On the morning of day 10 of gestation (day 27 of treatment), C and T mice were killed by cervical dislocation to study the differentiation, viability, growth, and morphology of embryos exposed to ethanol consumption. A total of 36 females for the control group and 38 females for the ethanol-treated group were used.

In separate trials, eight pregnant mice were treated with ethanol 10% for 17 days previous to gestation, superovulated and mated, and then continued to be administered ethanol solution in drinking water up to day 10 of gestation, as described above. On day 10 of gestation (day 27 of ethanol treatment), they were decapitated at 6:00 AM (time point corresponding to

the end of the dark period of the light–dark cycle) and trunk blood was collected into heparinized *Eppendorf* tubes. The same procedures were carried out on five CF. Samples were held at 4°C for blood ethanol measurement within 4 hr of collection to obtain supernatant for NAD/NADH enzymatic assays by a commercial kit (sensibility = 0.1 mg/dl).

Embryo Collection at Organogenic Period

In the morning of day 10 of gestation, control and periconceptionally ethanol-treated females were killed by cervical dislocation. Abdominal cavities were surgically opened, and uteri were quickly removed and placed in Petri dishes with Krebs-Ringer Bicarbonate solution (KRB): 11.0 mM glucose, 145 mM Na^+, 2.2 mM Ca^{++}, 1.2 mM Mg^{++}, 127 mM Cl^-, 25 mM HCO^{3-}, 1.2 mM SO_4^{2-} and 1.2 mM PO_4^{3-}. Under a stereomicroscope (Wild Heerbrugo Photomakroskop M400, 2×), implantation sites (IS) were isolated to be immediately fixed in paraformaldehyde 4% for embryo histopathological analysis and immunohistochemistry. Myometrial and decidual tissues were removed to release the conceptuses and then embryos were dissected from their extra-embryonic membranes to analyze organogenic development (differentiation, resorption rate, vitality, morphology, and growth). Immediately they were fixed for scanning electron microscopy or immunohistochemical assays or stored at −70°C for western blot.

CF-1 Embryo Differentiation Staging on Day 10 of Gestation

Isolated embryos were observed under stereomicroscopy and classified by their differentiation status. Classification and indexation of embryo differentiation stages was performed according to the Theiler system (TS: Theiler stage scale) described for (C57/BL × CBA) F1 hybrid mice (Kaufman and Bard, 1999). It is based on external appearance (NT, body flexure, forelimb buds, number of branchial arches, and number of somites. Considering that mating takes place at the mid-dark point, the first stage of embryo differentiation (E1) was established when vaginal plug appeared on the following morning.

We evaluated mean percentages of embryo differentiation of the total number of IS derived from each female (embryo variations within litters), the mean embryo number per female (variations between litters), and the total embryo number of IS recovered (frequency [%] of embryo stages).

Organogenic Embryo Viability Evaluation

Vitality of the embryo was evaluated by the presence or absence of heartbeat, when beating was first observed at the E9.5 stage. Viability was calculated as the mean number of live embryos staged at E9.5 to E10.5 of the total IS or of the number of females analyzed (variations within and between litters, respectively).

External Organogenic Morphological Stereomicroscopic Evaluation

The morphology of embryos staged at E9.5 to E10.5 was studied under a stereomicroscope (Wild Heerbrugo Photomakroskop M400). Principal observations carried out were neural fold formation, closure of NT, and turning of the embryo. Numbers and percentages (%) of abnormal embryos in E9.5 to E10.5 stages were calculated by considering the number of IS per female or the number of females analyzed in each group. The mean embryo percentage of the number of IS for each female represented variations within litters and the mean embryo number of the number of females represented variations between litters. The frequency of total abnormal embryos or abnormal types of the number of IS containing E9.5 to E10.5 embryos was also recorded.

Scanning Electron Microscopy and Morphometric Analysis

Embryos at organogenic stages were removed from extraembryonic membranes, classified as E10 and E10.5 stage, and separated for fixation in 2.5% glutaraldehyde (Sigma Chemical Co.) in phosphate buffer saline (PBS, 1×) (pH 7.4) for at least 24 hr at 4°C. Following fixation, embryos were rinsed in PBS and deionized water, dehydrated in acetone (30–50–70–90 and 100%), and dried in acetone: hexamethyl disilizane (Sigma Chemical Co.) (1:1) for 30 min. Embryos were mounted on aluminum stubs, then sputter coated with silver palladium (Bal-Tec-SCD-050), viewed and photographed at 15 kV with a JEOL-SSM 35CI scanning electron microscope. Embryo morphometry was performed on lateral digitalized embryo images and processed by Image-Pro Plus. The following embryonic measurements (μm) were made: Length 1 (L1): crown-rump length; L2: lateral cephalic (craniofacial) length (prosencephalic–rhombencephalic rims); L3: mesencephalic–first branchial arch length; L4: rhombencephalic rim–first branchial arch length; L5: mesencephalic–nasal prosencephalic length. Relative growth of the cephalic region in relation to the body was analyzed as length of cephalic size (L2) over L1. Morphometric analyses were performed on 5 litters (dams) of control and ethanol-treated groups.

Organogenic Embryonic Protein Mass Determination

The growth of organogenic embryos staged at E9, E10, and E10.5 was evaluated by direct measurement of protein content. Briefly, each embryo was separated from yolk sac and sonicated in 500 μl of 0.5 M NaOH, refrigerated and assayed by the method of Lowry et al. (1951). Data were expressed as μg protein/embryo.

Histology

For embryo histological analysis, IS were fixed in 4% paraformaldehyde/PBS for 3 hr at 4°C, dehydrated and embedded in Paraplast. Transverse central sections of the IS containing a whole embryo in the cavity were performed by cutting (7 μm thick) perpendicularly to the longitudinal axis of the uterus so as to include the largest area of decidua. Slices were deparaffinated in xylene, hydrated through decreasing concentrations of ethanol, and stained with Hematoxylin and Eosin (H-E) according to standard protocols. Specimens were analyzed and photographed using an Axiophot Zeiss microscope (Carl Zeiss, Inc. Oberkochen, Germany) equipped with a video camera on line with a Nikon image analyzer. General embryo histopathology, cephalic NT, somites, and mesodermal tissues were evaluated.

At least two IS containing an E10 to E10.5 embryo from each female were analyzed in a total of five females for each group.

Hoechst 33,342 Staining

Deparaffinated sections of IS with E10 to E10.5 embryos from control and ethanol-treated groups were rinsed three times in PBS and incubated in a Hoechst 33,342 solution (0.5 μg/ml in PBS). After further rinses in PBS, sections were coverslipped with a solution containing glycerol 30% in PBS and photographed with an Axiophot Zeiss microscope (Carl Zeiss, Inc.). Normal and/or abnormal nuclei were identified on the basis of morphologic pattern.

Immunohistochemistry

Immunohistological analyses were performed to detect N- and E-cadherin expression on organogenic E10 embryos. Tissue paraffined sections were deparaffinated and rehydrated through a graded series of ethanol solutions and finally washed three times in PBS for 5 min each. Then slices were heated in 10 mM sodium citrate in PBS, pH 6.0 in microwave (5 min at 370 W) and cooled in PBS. Sections were permeabilized with PBS-Triton 0.25% for 15 min. After washing in PBS (3×5 min), endogenous peroxidase activity was blocked in 3% hydrogen peroxide/PBS for 30 min at room temperature (RT). Then sections were washed (PBS, 3×5 min) and incubated in normal horse serum (NHS) (1:40) in PBS at RT in a humid chamber for 1 hr. They were incubated with primary antibodies against N-or E-cadherin (1:100) (mouse monoclonal antibodies; BD Pharmingen, San Diego, CA) and diluted in NHS (1:40) overnight at 4°C. After three washes (5 min each), sections were incubated with biotinylated horse monoclonal antibodies against mouse IgG (1:100) (Vector Laboratories, Burlingame, CA) in NHS (1:40) for 1 hr at RT. They were washed (3×5 min) and the reaction was enhanced with streptoavidin, horseradish peroxidase-conjugated (Chemicon International Inc., Temecula, CA) (1:300) in NHS (1:40) for 1 hr incubation at RT. Finally, samples were washed (3×5 min) and treated for 2 min with 3-3′-diaminobenzidine in chromogen solution (Dako kit). Slides were counterstained with hematoxylin and mounted in DPX. They were observed and photographed with an Axiophot Zeiss light microscope (Carl Zeiss, Inc.) equipped with a video camera on line with a Nikon image analyzer. Specificity of staining was determined by incubating sections with NHS (1:40) in the absence of the first antibody.

Embryonic Protein Extraction for Western Blot

To evaluate cadherin expression on organogenic embryos by western blot, −70°C-stored E10 embryos were prepared as follows. Protein from six to eight embryos per sample was extracted by homogenization in 100 μl of ice-cold Lysis Buffer containing 50 mM Tris–HCl (pH 7.4), 1% NP-40, 1 mM EDTA, and 1 μl of protease inhibitor cocktail (Sigma Chemical Company). Samples were placed on ice for 30 min and then crude homogenates were centrifuged at 13,000 rpm for 15 min at 4°C. The supernatant was stored at −70°C. Protein content was determined by the Bradford assay (Bio-Rad, Hercules, CA).

Western Blot

Extracts were dissolved with sample buffer (500 μM Tris–HCl, pH 6.8, 10% SDS, 30% glycerol, 0.5% β-mercaptoethanol, and 0.5% bromophenol blue), boiled for 5 min, and immediately placed on ice. Equal amounts of proteins (~40 μg/lane) under reducing conditions were resolved on 10% SDS-polyacrylamide gel (SDS-PAGE) (10% acrylamide/bisacrylamide for the resolving gel and 5% acrylamide/bisacrylamide for the stacking gel) in Mini Protean Cell (Bio-Rad). After SDS-PAGE, they were equilibrated in transfer buffer for 15 min and electrotransferred at 150 V for 90 min at constant voltage onto nitrocellulose membranes (Sigma Chemical Co.) using a mini trans-blot cell (Bio-Rad). Transfer was monitored by Ponceau red staining and membranes were blocked with 5% nonfat dry milk in PBS-Tris containing 0.1% Tween 20 (PBS-T) for 90 min. For immunoblotting, we used mouse anti N-cadherin (BD) (1:1000), mouse anti E-cadherin (BD) (1:500) and as load control, rabbit anti-β-actin (Sigma Chemical Co.) (1:4000) diluted in blocking buffer. They were incubated for 20 hr at 4°C. Blots were washed and incubated with secondary biotinylated-horse antimouse and secondary biotinylated goat antirabbit (Vector Laboratories) (1:6000) for 2 h at RT. After washing (PBS-T), the reaction was enhanced with streptoavidin, horseradish peroxidase-conjugated (1:7000) (Chemicon International Inc.) for 1 hr incubation. Blots were revealed by the chemiluminescence system using ECL Western blotting system (GE Healthcare, Uppsala, Sweden). Prestained protein standards (Bio-Rad) with a molecular weight range of approximately 199.7 to 6.7 kDa were used. Autoradiographic band intensities were quantified by densitometry (Scn Image Program). As negative control, normal IgG primary antibody was omitted. Western blots were performed at least three times on a total of seven control and six experimental embryonic samples. The intensity of each N- and E-cadherin band was relativized to the actin band and expressed as mean protein arbitrary units (AU) (±SD).

Statistical Analysis

Reported values represent the mean ± standard error (SE) or standard deviation (SD) of control and ethanol-treated groups. Differences between the means of groups were statistically analyzed by one-way analysis of variance (ANOVA) and Mann–Whitney test. Values of frequency were compared by Fisher's exact test. When appropriate, a two-tailed Student's *t*-test was performed for each pair of results. For statistical analysis, we used the GraphPad Instat v2.05a (GraphPAD software Inc., San Diego, CA). Statistical significance was $p < 0.05$.

RESULT

Mouse Weight, Food and Liquid Consumption, and Blood Ethanol Concentration

There were no weight differences between the groups before and after ethanol exposure. At the beginning of the ethanol administration period, mice weighed 28.5 ± 1.2 and 27.1 ± 0.8 g for control and ethanol-treated group, respectively. By the end of the periconceptional

period, weights were 29.5 ± 1.2 g for control and 29.1 ± 0.8 g for ethanol-treated group. During the ethanol exposure period (27 days), ethanol-treated mice drank a mean of 185.7 ± 10.6 ml/kg/day (5.2 ± 0.3 ml/mouse/day) of ethanol. This represents an ethanol-derived calorie (EDC) intake of approximately 131.8 ± 7.4 kcal/kg/day, which constituted 18.0% EDC of total daily calorie intake. There were no differences in the daily pattern of food intake between the two groups. Total calorie intake in control and ethanol-treated groups was similar: 693.3 ± 64.3 and 729.2 ± 69.7 kcal/kg/day, respectively.

Blood alcohol concentration (BAC) in ethanol-treated females varied between 16 and 40 mg/dl at the end of exposure. The mean BAC value on day 27 of exposure to 10% ethanol intake was 24.5 ± 5.04 mg/dl. In control animals, BAC was undetectable.

CF-1 Mouse Embryo Differentiation and Viability After Periconceptional Ethanol Exposure

The embryonic stages of differentiation found on day 10 of gestation in both control and ethanol-treated females are shown in Figure 1. The E7 to E7.5 gastrulating embryo has an incipient neural plate (Fig. 1A). At E8 to E8.5 stage, the embryo presents the neural plate that develops into neural folds at the anterior part (Fig. 1B), and at E9 stage, the unturned embryo have one to seven somites and a nonbeating heart (Fig. 1C). At E9.5 stage (8 to 10 somites), the neural folds begin to fuse and a beating cardiac tube is evident (Fig. 1D). At E9.75 stage (11 to 13 somites), the NT has expanded (Fig. 1E), whereas at E10 stage the turned embryo (14 to 20 somites) has the cephalic NT closed or in apposition but not at the posterior neuropore. The forelimb buds and the first and second branchial arches become evident (Fig. 1F).

The embryo stages of differentiation reached at day 10 of gestation were quantified in the control and ethanol-exposed group. In control CF-1 mice, the highest quantities of embryos were found at E10 and E10.5 stages, both within and between litters (Table 1). In ethanol-exposed females (EF), the mean percentage or number and frequency of E10to E10.5 embryos was significantly lower compared with controls ($p < 0.01$, $p < 0.001$) (Table 1). Although the frequencies of E8 to E9.75 embryos from EF were significantly higher compared with controls, the mean percentage or number of embryos within litters or between females was not different from controls (Table 1).

Reabsorbed IS contained retarded embryos staged at E7 to E8.5 with necrotic and/or hemorrhagic trophoblast-decidual tissue. A very significantly increased resorption percentage was found in the ethanol-exposed group compared with controls ($p < 0.05$, Mann–Whitney test, $p < 0.001$, Fisher's test, Table 2) while the mean quantities of delayed embryos (unturned E9 plus E9.5 embryos with 8–10 somites) were significantly higher in the exposed group ($p < 0.05$, Mann–Whitney test; $p < 0.001$, Fisher's test, Table 2). The embryo viability (the number of embryos with positive heartbeat) resulted significantly lower in the ethanol-exposed group compared with the percentage of the control group ($p < 0.001$; Table 2).

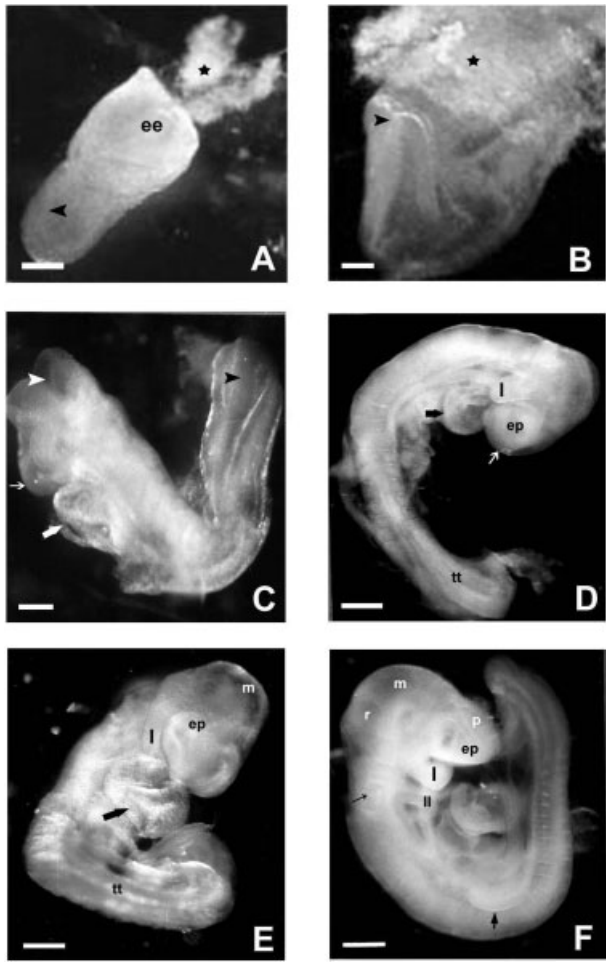

Fig. 1. Embryo differentiation on day 10 of gestation in CF-1 control and ethanol-exposed mice. At organogenic period of gestation, different stages of differentiation (E) in the two groups studied. Stereomicroscope micrographs of staged embryos are presented for anatomical references. (**A**) E7 to E7.5, (**B**) E8 to E8.5, (**C**), E9, (**D**) E9.5, (**E**) E9.75, and (**F**) E10. *Trophoblast tissue, arrowhead: anterior ectoderm (neural plate in E7 and neural fold in E8). ee, extraembryonic ectoderm. In E9, white arrowhead: cephalic neural fold, black arrowhead: posterior NT (open neuropore), thin arrowhead: prosencephalon, and thick arrowhead: heart. In E9.5, ep: epibranchial placode (optic vesicle), tt: turning tail. I: first branchial arch. Heart and prosencephalon are indicated by arrows. In E9.75, m: mesencephalon. In E10, p: prosencephalon, m: mesencephalon, r: rhombencephalon, ep: epibranchial placode, I: first branchial arch, II: second branchial arch, arrow: otic pit, short arrow: forelimb bud. Scale bar A, B, C, D: 100 μm, scale bar E and F: 200 μm. NT, neural tube.

Effect of Periconceptional Ethanol Exposure on Embryo Growth in the Organogenic Period

We studied the organogenic (E10–E10.5) embryo growth by the measurement of E10 embryo size by scanning image analysis. The body length (crown-rump length, L1) and length sizes (L2–L5) of cephalic region were shown in Figure 2A and B. The crown-rump and L2 to L5 lengths of ethanol-exposed E10 and E10.5 embryos were significantly reduced compared with that of control-derived embryos ($p < 0.01$ and $p < 0.001$, respectively) (Table 3A and B). After length size

Table 1
Embryo Differentiation on Day 10 of Gestation in CF-1 Murine Strain

Group			E<7.5	E8–8.5	E9	E9.5–9.75	E10–10.5
Control	Female Nr	36					
	Total IS Nr	491					
	Mean IS/Fem (Nr)	13.6±0.9					
	Mean Emb/IS (%)		8.0±1.1	3.1±2.0	5.0±1.0	10.0±2.0	72.2±2.6
	Mean Emb/Fem (Nr)		1.0±0.2	0.1±0.07	0.7±0.2	1.22±0.3	10.4±1.1
	Total Emb Nr		37	6	24	44	374
	Total Emb (%)		7.5	1.2	4.8	8.9	76.1
Ethanol treated	Female Nr	38					
	Total IS Nr	429					
	Mean IS/Fem (Nr)	11.3±0.6*					
	Mean Emb/IS (%)		21.1±4.0*	2.1±1.0	10.1±2.0	13.1±2.1	52.3±3.0**
	Mean Emb/Fem (Nr)		2.2±0.4*	0.2±0.1	1.2±0.3	1.6±0.3	5.9±0.7**
	Total Emb Nr		84	9	46	62	227
	Total Emb (%)		19.5***	2.1	10.7***	14.4****	52.9***

Embryos from control ($n = 36$) and ethanol-exposed ($n = 38$) females were dissected on day 10 of gestation and classified for differentiation stages as described in materials and methods. We evaluated the total Nr of IS, the mean IS Nr per female (±standard error (SE), the mean embryo percentage over the total IS Nr in each female (±SE) (variations within litters), the mean embryo Nr per female (±SE) (variations between litters), and the frequency of embryos over the total IS Nr from control and treated group (%). *$p<0.05$, **$p<0.01$ vs. control group, Mann–Whitney test. ***$p<0.001$, ****$p<0.01$, vs control group, Fisher's exact test. Nr, number; IS, implantation sites.

Table 2
Embryo Resorptions, Delayed Development, and Vitality

	Control group	Ethanol-treated group
Female Nr	36	38
Total IS Nr	491	429
Mean resorptions/IS (%)	9.6±2.0	23.5±4.3*
Mean resorptions/Fem (Nr)	1.2±0.2	2.5±0.4*
Nr resorptions	43	93
% Resorptions	8.7%	21.6%**
Mean delayed Emb/IS (%)	8.2±2.4	14.1±3.3*
Mean delayed Emb/Fem (Nr)	0.9±0.2	1.8±0.2*
Nr delayed Emb	34	66
% Delayed Emb	6.9%	15.3%**
Mean viable Emb/IS (%)	81.1±0.3	59.2±0.5***
Mean viable Emb/Fem (Nr)	11.3±1.0	6.7±0.6****
Nr viable Emb	409	258
% Viable Emb	83.2%	60.1%**

Embryo resorptions were assessed as the total Nr of embryos at stages E6 to 8.5. Delayed and nonviable embryos were E9 plus abnormal E9.5 ones with 8to 10 somites, open neural tube. Viable embryos were recorded from E9.5 to 10.5 stages, with positive heartbeat. Means embryo % or Nr (±SE) (variations within or between litters, respectively) and total embryo Nr over total IS Nr were recorded in control and ethanol treated groups. *$p<0.05$, ***$p<0.01$, ****$p<0.001$ vs. control group, Non-parametric analysis, Mann-Whitney test. **$p<0.001$ vs. control group, Fisher's exact test. Nr, number; IS, implantation sites.

normalization respect to the control value ones, all length sizes of E10 or E10.5 embryos of the ethanol-exposed group resulted diminished (Fig. 3). The proportion of brain size (L2) vs. body size (L1) was evaluated. Although at E10 stage the ethanol-exposed embryos did not show changed in cephalic proportion as compared with the control ones (51.8±1.5 vs. 52.0±4.0, respectively), the ethanol-treated derived embryos at E10.5 stage had significantly reduced proportional cephalic size vs. controls (44.5±1.6 vs. 51.0±2.1, respectively, $p<0.05$).

Protein content (a degree of embryo growth) of control-derived embryos was linearly progressive and increased with the somite number, according to the development of the embryonic stages (E9: 28.7±3.8; E9.5–E9.75: 39.4±4.1; E10: 62.9±3.3; E10.5: 91.1±4.7 μg protein/embryo). Although ethanol-exposed derived embryos showed a similar linear pattern of protein levels up to E10 stage, the E10.5 embryos had significantly reduced protein content compared with the E10.5 embryos of the control group (81,5±3.1 vs. 91,1±4.7, $p<0.05$).

Effects of Periconceptional Ethanol Exposure on Organogenic Embryo Morphological Parameters

Figure 4A showed normal apposed/closed NT with visible first and second branchial arches. The main gross abnormalities found in turned embryos were abnormal closure of cephalic NT, observed as asymmetrically fused neural folds in the prosencephalic–mesencephalic region

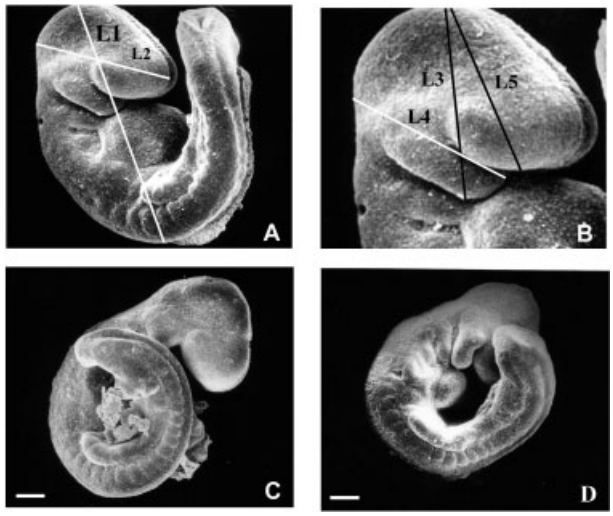

Fig. 2. Scanning morphological analysis of organogenic E10 to E10.5 embryos. Scanning electron micrographs of whole E10 embryo (**A**) and embryo external craniofacial region (**B**) are provided for anatomical reference. (A) Illustration of a lateral view of control mouse embryo indicates location of crown-rump length (L1) and craniofacial length (prosencephalic–rhombencephalic rims) (L2). (B) Lateral view of cephalic region indicating the different lengths: L3: mesencephalic–first branchial arch length; L4: rhombencephalic rim–first branchial arch length; L5: mesencephalic–nasal prosencephalic length. (**C**) Lateral view of control E10 embryo. (**D**) Lateral view of ethanol-exposed E10 embryo. Note difference of body size vs. control embryo. Scale bar: 100 μm.

Table 3
Embryonic Growth Analysis in E10 Organogenic Embryos

Group	L1	L2	L3	L4	L5
A. E10 embryo stage					
Control	1201.2±31.2	598.4±31.5	555.3±25.5	471.2±18.8	537.5±21.3
Ethanol-treated	712.8±62.1**	352.9±32.6**	355.8±26.7**	281.5±28.5**	323.3±24.8**
B. E10.5 embryo stage					
Control	1693.0±105.5	933.5±65.6	799.8±21.5	740.0±29.4	754.3±35.1
Ethanol-treated	853.5±19.9***	378.5±14.9***	412.8±8.7***	301.2±23.1***	335.6±24.1***

Embryo growth was assessed by evaluation of different embryonic lengths (L) as described in materials and methods. Data represent the mean length Nr/litter (μm)±SE (five animals in each group). $^{**}p<0.01$, $^{***}p<0.001$ vs. control group, Student's *t*-test.

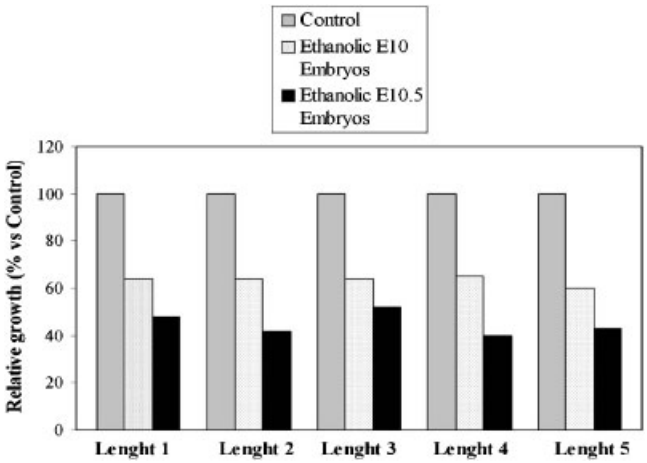

Fig. 3. Relative growth of ethanol-exposed embryos vs. control embryos. The percentages of reduction of lengths (L) of ethanol-exposed embryos were normalized to control embryo sizes and analyzed in E10 and E10.5 embryo stages. L1: crown-rump length, L2: prosencephalic–rhombencephalic rims length, L3: mesencephalic–first branchial arch length, L4: rhombencephalic rim–first branchial arch length, L5: mesencephalic–nasal prosencephalic length.

(Fig. 4B), as fully open NT (Fig. 4C) or partially open NT at the rhombencephalon (Fig. 4D) or at the prosencephalon (Fig. 4E).

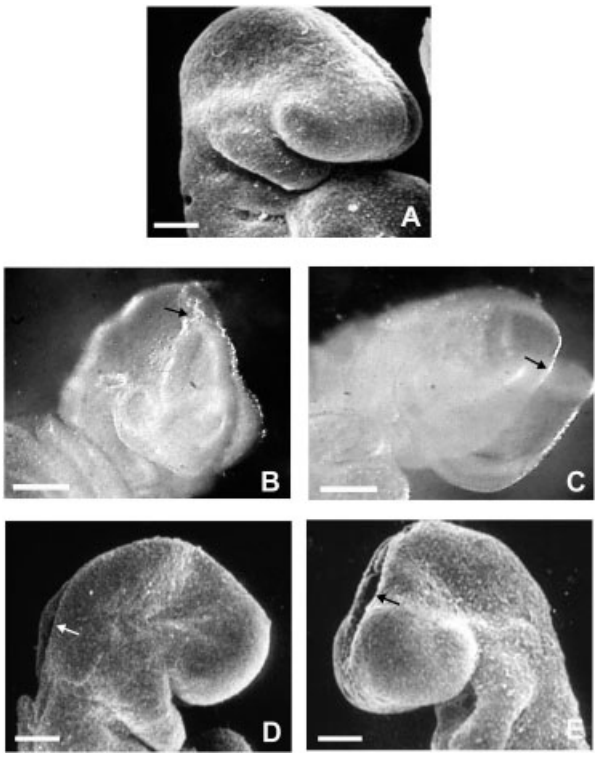

Fig. 4. Morphology of cephalic NT in E10 to E10.5 embryos. Scanning electron (**A**, **D**, and **E**) and stereomicroscopic (**B** and **C**) micrographs of cephalic NT closure (arrows) of organogenic staged embryos. (A) Normally closed cephalic NT. (B) Abnormally closed NT. (C) Severely open NT. (D) Partially open NT at rhombencephalon. (E) Partially open NT at prosencephalon. Scale bar: 100 μm. NT, neural tube.

The frequency, mean percentage, or mean number of morphologically abnormal organogenic embryos was significantly higher in the ethanol-exposed group compared with controls (Table 4). The mean percentage or number of abnormal E10 to E10.5 embryos was significantly elevated in the ethanol-exposed group compared with controls ($p<0.001$ and $p<0.01$, respectively), although the proportion of different types of abnormal E10 to E10.5 embryos (referring to open or abnormally closed NT) was similar in two groups (Table 4).

The ethanol-treated females had elevated proportions of embryos with altered cellular density (20%) and tissue disorganization (70%) (Fig. 5B) compared with the respective proportions of histological defects of control-derived embryos (3% or any) (Fig. 5A). Ninety percent of control-derived embryos had regular mesenchymal cells (Fig. 5C), whereas only 20% of ethanol-exposed embryos had normal mesenchymal characteristics. They presented irregular cell shapes with slightly reduced sizes and lower cellular mesodermal density (Fig. 5D and 5E vs. C). The ethanol-exposed embryos had abnormal somite formation, at the inner cell layers, compared with that of the control-derived embryos (Fig. 5G–I vs. 5F and H). Neuroectodermal histopathology of each group is shown in Figure 6. Ethanol-exposed embryos had reduced neural lumen and thickened neuroepithelium (Fig. 6B) compared with control embryos (Fig. 6A). Increased proportion of spherical neuroepithelial cells, cellular dispersion, reduced cell adhesion, and tissue disorganization was found in ethanol-exposed embryos (Fig. 6D and F) compared with neuroepithelium of control embryos (Fig. 6A, C, and E). In control embryos, sufficient neuroepithelial surface of neural fold contacts (Fig. 6E). In contrast, the apposed NT of ethanol-exposed embryos had thin neuroepithelial neural folds with asymmetric growth (Fig. 6F). Nuclear defects, distribution, organization, and nuclear density were subjected to nuclear analysis in Hoechst-stained sections. Higher proportion of pyknotic nuclei (reduced nuclear size and

Table 4
Ethanol Effects on Morphology of E9.5 to E10.5 Embryos

	Control group	Ethanol-exposed group
Female (Nr)	36	38
IS (Nr)	418	289
Mean abnormal Emb (%)	12.38 ± 2.57	45.05 ± 4.41*
Mean abnormal Emb (Nr)	1.41 ± 0.29	3.27 ± 0.43*
Total abnormal Emb (Nr)	51	124
Total abnormal Emb (%)	12.20	42.91**
Mean abnormal E9.5–E9.75/IS (%)	2.64 ± 1.87	7.67 ± 3.06
Mean abnormal E9.5–E9.75/Fem (Nr)	0.27 ± 0.20	0.53 ± 0.24
Total abnormal E9.5–E9.75 (Nr)	10	20
Total abnormal E9.5–E9.75 (%)	2.39	6.92***
Mean abnormal E10–E10.5/IS (%)	9.74 ± 1.82	37.38 ± 4.59*
Mean abnormal E10–E10.5/Fem (Nr)	1.14 ± 0.23	2.74 ± 0.36 ****
Total abnormal E10–E10.5 (Nr)	41	104
Total abnormal E10–E10.5 (%)	9.81	35.99**
Open NT (%)	27/41 (65.85)	59/104 (56.73)
Abnormal closed NT (%)	14/41 (34.15)	45/104 (43.27)

Abnormal external morphological characteristics of organogenic embryos, mainly development and closure of the NT, were taken account in both groups. Abnormal organogenic embryos at E9.5–E9.75 plus E10–E10.5 stages were quantified within litters (% ± SE) and between litters (Nr ± SE). Frequency of abnormal embryos (Nr and %) with open NT or abnormally closed NT were also recorded. ****: $p<0.01$, *: $p<0.001$ vs. control group, Mann–Whitney test. **$p<0.001$, ***$p<0.01$ vs. control group, Fisher's exact test. NT, neural tube; IS Nr, total implantation site number.

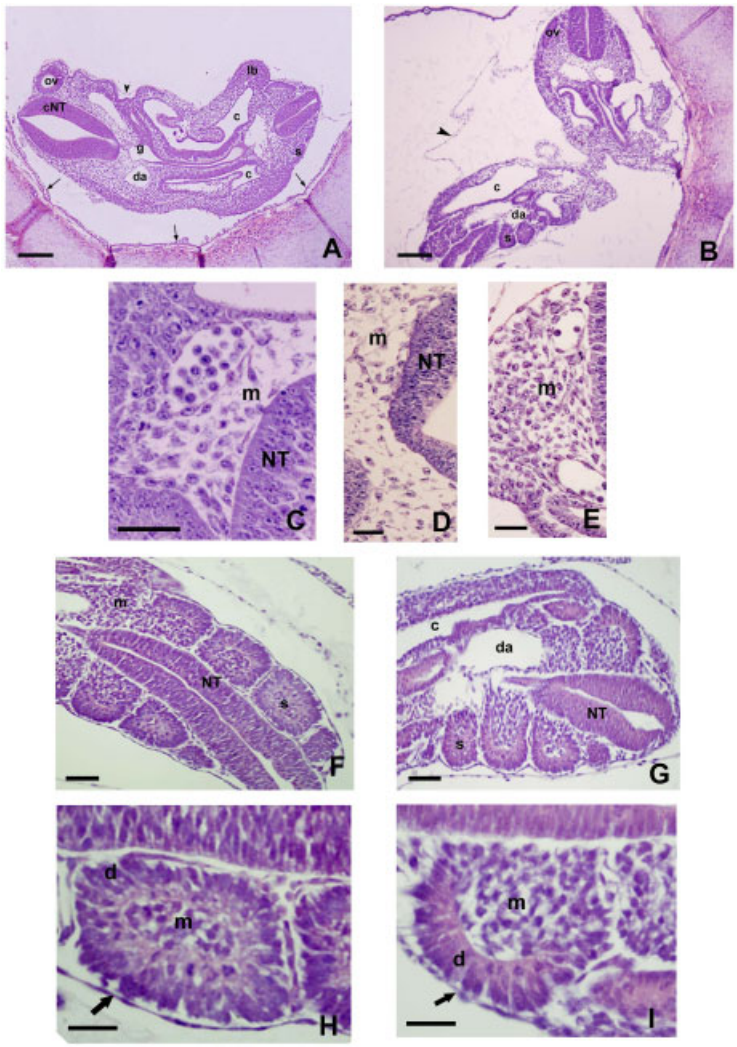

Fig. 5. Histopathology of E10 organogenic embryos. Effects on mesoderm and somite development. Histological sections of control (**A**, **C**, **F**, and **H**) and ethanol-exposed (**B**, **D**, **E**, **G**, and **I**) E10 embryos stained with hematoxylin and eosin. Cell adhesion alterations and tissue disorganization are observed in the whole ethanol-exposed embryo (B) vs. control embryos (A). (C, D, and E) Mesenchymal tissue. Note the irregular shapes and sizes of mesenchymal cells and altered cell density evident in mesoderm of ethanol-exposed embryos (D and E) vs. mesodermal tissue of control embryos (C). (F, G, H, and I) Somite development. Details of incomplete somite development in ethanol-exposed embryos (G) vs. somites of controls (F) are shown in I vs. H, respectively. cNT, cephalic neural tube; ov, optic vesicle; c, coelom; g, gut; da, dorsal aortae; lb, limb bud; s, somite; m, mesenchyme; d, dermatome; m, myotome. Arrows: yolk sac; arrowhead: amnion. Thick arrow: epidermis. Scale bar A and B: 100 μm; bar C, D, E, F, G: 50 μm; bar H and I: 25 μm.

high fluorescence intensity), cells with irregular shape or nuclear fragmentations, and abnormal density and nuclei organization were found in mesoderm of ethanol-exposed embryos, whereas control-derived embryos had homogenously and regularly distributed ovoid–polyhedral mesodermal nuclei. The nuclei of somites of control-derived embryos were interphasic nuclei, whereas ethanol-exposed embryos presented a larger proportion of morphologically irregular nuclei with high chromatin condensation and desorganization. Concerning the nuclei of neuroepithelium, in contrast to the elongated nuclear shapes and columnar organization of neuroepithelial tissue of control-derived embryos, ethanol-exposed embryos had pyknotic nuclei and displacement of neuroepithelial nuclei from the ependymal layer toward the marginal layer, producing increased nuclear density close to mesodermal tissue.

E- and N-cadherin localization and distribution patterns were analyzed in E10 embryos. E-cadherin was localized in the epithelium of epidermis, oral cavity, aortic archs, pharynx, and pericardial cavity but not in mesenchyme, in both control and ethanol-exposed groups (Fig. 7A and B). E-cadherin was also detected in heart membranes of ventricle of control (Fig. 7C) and ethanol-exposed embryos (Fig. 7D). N-cadherin immunoexpression was detected in heart and NT of control (Fig. 8A) and ethanol-exposed embryos (Fig. 8B). The levels of E- and N-cadherin expression were analyzed by western blotting (Fig. 9). Ethanol-exposed embryos presented significantly increased E- and N-cadherin expression compared with the same molecules of control-derived embryos embryos ($p < 0.05$; Fig. 9A and B).

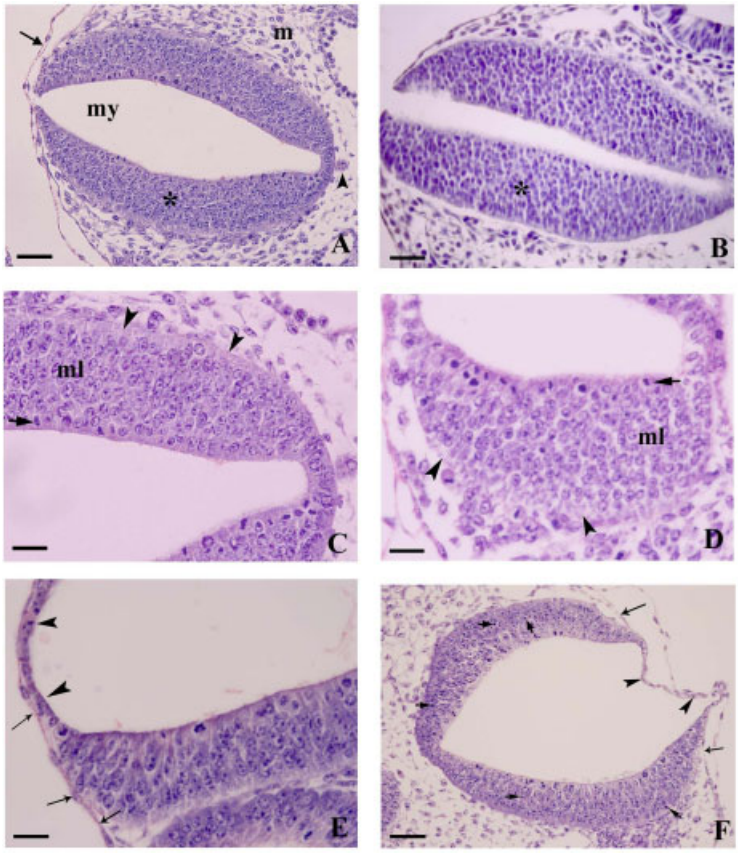

Fig. 6. Histopathological effects on NT of E10 embryos. Histology of cephalic NT of control (**A**, **C**, and **E**) vs. ethanol-exposed (**B**, **D**, and **F**) embryos was evaluated. Reduced neural lumen and neuroepithelial thickness is observed in ethanol-exposed embryos (B) vs. NT of control embryos (A). Increased spheric neuroepithelial cells with reduced sizes, decreased adhesion, and neuroepithelial tissue disorganization, particularly in the marginal layer, are evident in NT of ethanol-exposed embryos (D) vs. NT of controls (C). (E and F) Detail of neural tissue at the roof level of both hemispheres. It clearly indicated neural tissue growth at roof (arrowheads) and epidermis (arrows) near the roof plate in NT of control (E) and ethanol-exposed embryos (F). Observe abnormal and partial NT closure with thin neuroepithelial tissue and pyknotic nuclei (arrows) located at the mantle layer of rhombencephalon (F). In A and B, m: mesenchyme; my: myolocoel, *neural tissue. Arrow: amnion; arrowhead: notochord. In C and D, ml: mantle layer; arrowheads: marginal layer, arrows: ependymal layer. In E and F, arrowheads: neural tissue; arrows: epidermis; short arrows: pyknotic nuclei. Scale bar A, B, and F: 50 μm; scale bar of C, D, and E: 25 μm. NT, neural tube.

DISCUSSION

The findings of this study show that moderate periconceptional ethanol consumption up to midgestation in CF-1 mouse exerted deleterious effects on embryonic differentiation, growth, and morphology. Concomitantly with morphological embryonic damage characterized by histological alterations and NT closure defects, ethanol exposure induced upregulation of E- and N-cadherin expression. To our knowledge, these results are the first report on teratogenic effects of periconceptional ethanol exposure to organogenic CF-1 embryos.

In this study, we presented a mouse model for studying the maternal ethanol effects in which subtle sequellae of insult during early stages of organogenesis can be generated with BAC of 24.5 mg/dl. It is well known that the severity of ethanol's effects and maternal BAC varies with the route of administration, the dose and period of ethanol exposure (Simpson et al., 2005). To better model the human experience in terms of route of ethanol administration and BACs achieved, an oral ethanol exposure paradigm was utilized in this study. Although most reliable measure of fetal or maternal exposure to ethanol is BAC, this variable is rarely known in human studies. However, examination of BACs achieved in many animal models facilitates some comparison with human situation. For example, the peak of BACs in dams consuming about 36% EDC was between 50 and 100 mg/dl that was generally considered to correspond to heavy drinking, whereas peak BACs lower than 50 mg/dl (with 25% EDC) represent moderate drinking (Simpson et al., 2005). In general, animal models for acute ethanol exposure, which induces several embryo-fetal malformations depending of the period of gestational exposure, produced BAC in the range of 100 to 400 mg/dl (Kotch and Sulik, 1992a). Models for chronic exposure (before mating and during pregnancy or up to specific embryo stages, and/or during lactation) usually lead to BACs between 65 and 220 mg/dl (Amini et al., 1996; Minana et al., 2000; Parnell et al., 2006; Boehm et al., 2009). Although the cited literature about BAC are very wide, here we demonstrated that perigestational moderate ethanol exposure in CF-1 mouse produce low BAC that is able to induce early abnormal organogenic embryo development.

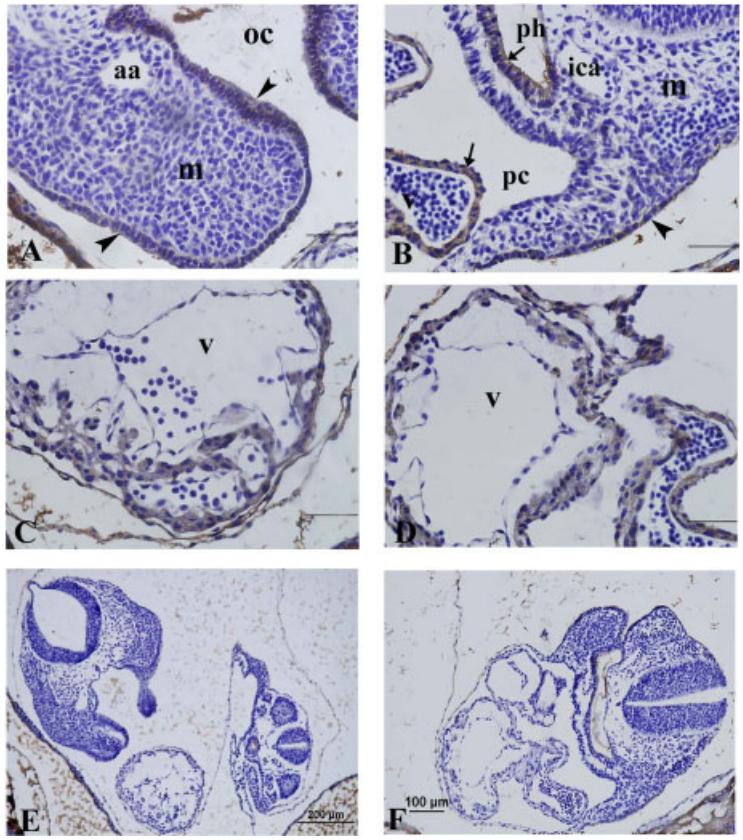

Fig. 7. E-cadherin immunolocalization in E10 to E10.5 embryos. Immunoreactivity for E-cadherin of embryonic organs at E10 stages of control (**A**, **C**, and **E**) and ethanol-exposed (**B**, **D**, and **F**) embryos is shown in the surface ectoderm (epidermis) (arrowheads) of oral cavity (oc), in the endocardium of ventricle (v), in the epithelium (arrow) of pericardial cavity (pc) and pharynx (ph). (E and F): Negative immunohistochemical embryo images of control and ethanol-exposed embryos. References of figures: m: mesenchyme; aa: aortic arch, ica: internal carotid artery; au: auricle. Scale bar A, B, C, D: 50 µm.

We first studied the vulnerability/sensibility of CF-1 embryos to periconceptional alcohol intake in relation to embryonic differentiation. This ethanol regimen did promote increased incidence of delayed embryo differentiation on day 10 of gestation manifested by reduced quantities of E10 to E10.5 embryos and increased E<7.5 embryo stages. The retarded embryonic differentiation, the reduced number of IS, and the increased reabsorption indicates that this ethanol regimen is able to produce embryo loss at early peri-implantation stages. Chronic ethanol intake at the time of conception and during pregnancy in humans has also been associated with increased risk of spontaneous abortion (Kesmodel et al., 2002; Herniksen et al., 2004). Although the exact causes are still unclear, alcohol is known to interfere with the normal functioning of the reproductive system by altering estrous cyclicity and prolactin and luteinizing hormone levels (Sanchis et al., 1985; Canteros et al., 1995; Cebral et al., 1998a). In another line, a possible cause of delayed-arrested differentiation of embryos at the organogenic period might be abnormal preimplantational embryo development (Wiebold and Becker, 1987). Alcohol exposure during preimplantation pregnancy was previously reported to reduce litter size by killing some embryos, causing delayed implantation of others and exerting adverse effects on decidualization in mice (Checiu and Sandor, 1981, 1982; Hunter et al. 1994). Ethanol-adverse effects can also be seen by increasing spontaneous activation of exposed mouse oocytes, defects that we observed after long-term ethanol exposure around ovulation (Cebral et al., 1998b, 2011). It was reported that haploid or diploid parthenogenetic embryos can develop more slowly than normal fertilized diploid embryos and survive at least up to day 10 of gestation but fail to reach the limb-bud stage while monosomic and trisomic embryos are capable of developing up to the morula stage (Kaufman and Bain, 1984a,b; Henery and Kaufman, 1992; Kaufman, 1997). In this respect, we think that embryo arrested-delayed differentiation at day 10 of gestation may be related to activation of oocytes during the periovulatroy period of exposure.

After periconceptional ethanol exposure, as organogenic development proceeds, the growth deficiency of the body and cephalic region seems to become more evident. E10.5 exposed embryos had more markedly reduced growth compared with E10 exposed embryos, suggesting that intrauterine growth retardation/restriction is manifested early at organogenesis (Lemoine et al. 1968; Allebeck and Olsen 1998). The reduced head of E10.5 embryos (the typically microcephaly of FASD) was presented together with hypoplasia of the first branchial arch (maxilar/mandibular prominence). These results seem to be similar to those found with maternal ethanol

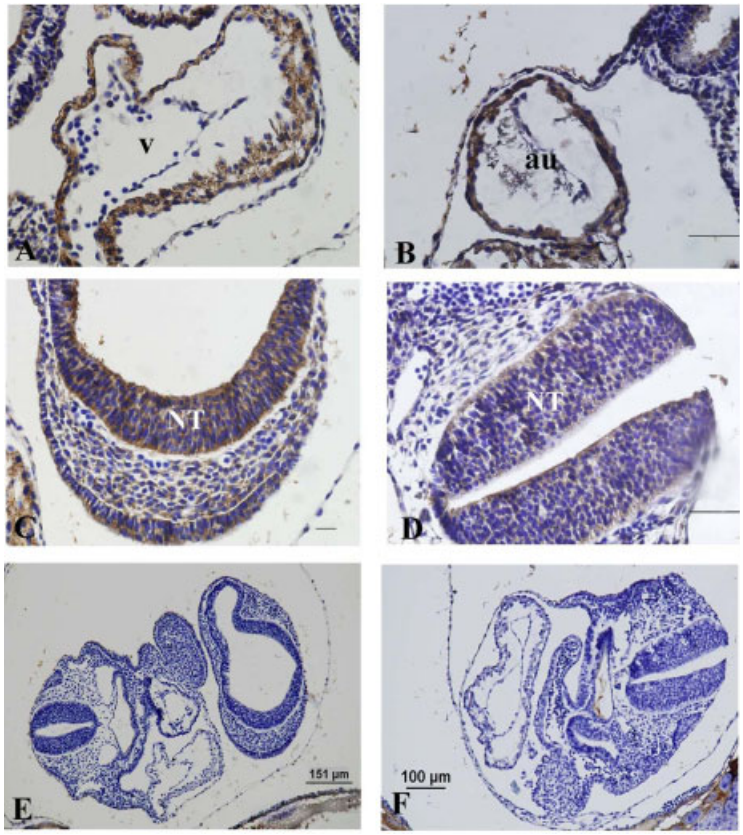

Fig. 8. N-cadherin immunolocalization in E10 to E10.5 embryos. Immunoreactivity for N-cadherin of embryonic organs at E10 stages of control (**A**, **C**, and **E**) and ethanol-exposed (**B**, **D**, and **F**) embryos is shown. Observe immunoexpression in endocardium of ventricle (v) and auricle (au) of both control (A) and ethanol-exposed (B) embryos. The neuroepithelium of the NT of ethanol-exposed embryos (D) showed reduced immunoreactivity vs. control NT (C). (E and F) Negative control sections of control and ethanol-exposed embryos, respectively. Scale bar: A and C: 20 µm; scale bar B and D: 50 µm. NT, neural tube.

treatment on day 7 or 8 of pregnancy in which median cleft lip and cleft palate, abnormalities of the eyes, brain, short palpebral fissures, and other fetal anomalies are found in other studies (Sulik et al., 1984). Alcohol-induced reduction of brain length and body size as well as hypoplasticity was also described in *Xenopus* embryos (Nakatsuji, 1983; Peng et al., 2004).

Retarded growth and dysmorphogenesis of the embryo may be interrelated, although they are not strictly dependent on each other since normal morphology can be found in an embryo with a reduced body size. In the present CF-1 mouse model, the mesodermal tissue of ethanol-exposed embryos was disorganized and had irregular mesenchymal cell shapes while ethanol induced alterations in somite development. Perturbation of cell population by ethanol could result in the cell condensation/pyknosis and dysmorphogenesis (Aoto et al., 2002). The NT was the embryonic organ most affected by ethanol exposure, at least in term of the quantities of embryos with defects of cephalic NT closure, as suggested by others (Mooney and Miller, 2007). In our model, one consequence of altered NT closure and narrow prosencephalon may be abnormal medial olfactory placode development. Similar to our results, reduced frontonasal prominence and asymmetric NT closure were also encountered after 12 hr of acute ethanol exposure of C57Bl/6J mouse embryos (Kotch and Sulik, 1992b). The neural lumen and NT closure, the neuroepithelial thickness, the tissue organization and the neural cell adhesion appeared to be negatively affected by ethanol exposure. At the time of NT closure, insufficient neuroepithelial surface of neural fold contact and asymmetric neural fold growth was detected in a large proportion of ethanol-exposed embryos. Increased nuclear defects, such us pyknosis, irregular shape, and/or nuclear fragmentations of ethanol-exposed embryos with anterior neural folds unclosed, suggested ethanol-induced neuroepithelial apoptosis. The hypothesis of excessive cell death particularly at the anterior neural fold perimeter was suggested to explain face and brain malformations (Dunty et al., 2001, 2002). It is feasible that ethanol acted directly on the neuroepithelium during the organogenic period, as suggested in other studies in which ethanol exposure during gastrulation stage causes enhanced cell death in the neuroepithelium and craniofacial regions (Kotch and Sulik, 1992a,b; Dunty et al. 2001, 2002; Da Lee et al., 2004). In any case, the window of vulnerability to ethanol-induced teratogenesis coincides with the time of neuronal generation (Miller, 1986, 2006) in which the lengthening of the cell cycle is one important adverse effect (Miller and Nowakowski, 1991).

The most common mechanisms proposed to explain delayed differentiation and dysmorphogenesis may be direct ethanol and/or acetaldehyde actions (Menegola et al., 2001; Lee et al., 2005). In neural cell cultures from 18 day-old rat fetuses, ethanol concentrations of

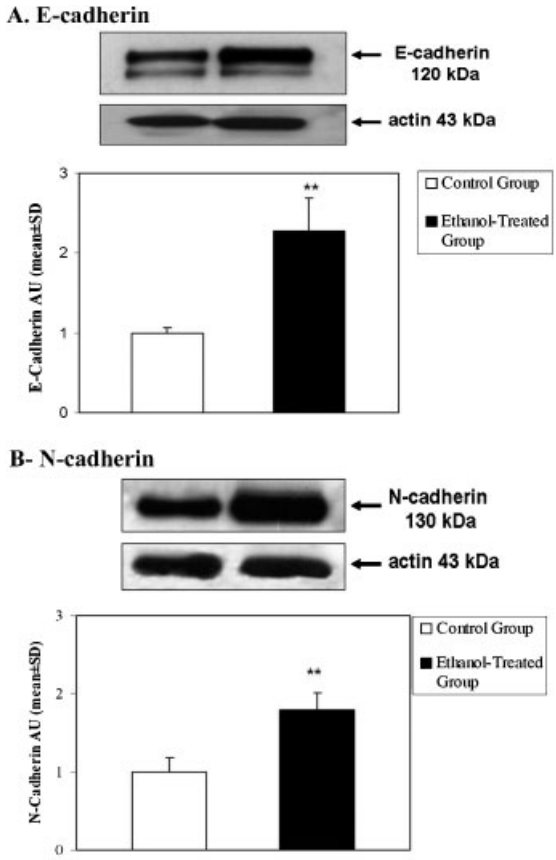

Fig. 9. E- and N-cadherin expression on organogenic advanced embryos. Western blot performed on E10 embryo extracts reacted with antibody to E-cadherin (**A**) and N-cadherin (**B**) found at the expected molecular size. Each band corresponds to one representative experiment out of three. Each band was quantified by densitometry using the Scieon Image program and expressed as AUs (mean ± SD). Graphic shows pooled data from three independent experiments. A significant increase in E-cadherin (A) and N-cadherin (B) expression in ethanol-exposed embryos compared with the control embryos was observed. $^{**}p < 0.01$, Student's *T*-test. AU, arbitary unit.

100 mmol/l led to DNA alterations (Lamarche et al., 2004). In vivo ethanol exposure affects signaling gene cascades and intracellular calcium concentrations (Debelak-Kragtorp et al., 2003), resulting in dysmorphogenesis and craniofacial abnormalities (Ahlgren et al., 2002). In this regard, two doses of 30 mg/kg of ethanol on day 7 of gestation in C75BL/6J mice perturb the expression of developmental genes inducing midline craniofacial malformations and holoprosencephaly (Higashiyama et al., 2007). Acetaldehyde, an inducer of DNA damage in multiple organs, can play an important role in ethanol neurotoxicity after ethanol exposure on day 7 of gestation (Kido et al., 2006) by acting directly on the developing nervous system and on microtubules and microfilaments of neuroepithelial cell. In spite of the many altered mechanisms proposed to be induced by alcohol, our work focused on alterations of cadherin expression in organogenic embryos after perigestational ethanol intake, since cadherin adhesion molecules are key determinants of morphogenesis and tissue architecture (Tunggal et al., 2005). Regulation of cadherin expression levels is crucial for the integrity of cell–cell junctions, tight junction formation, and cell differentiation (George-Weinstein et al., 1997; Sakamoto et al., 2008), remodeling and epithelial–mesenchymal transition during early morphogenesis (Savagner, 2001, Xu et al., 2001). In our mouse model, ethanol exposure did not affect localization or distribution of E- and N-cadherin in E10 embryos. N-cadherin was strongly expressed in NT and slightly in the apical side of the foregut and the surface ectoderm, whereas the expression of E- and N-cadherins was found in the heart primordium. In spite of similar immunoreactivity of E- and N-cadherinsin the two groups, increased embryonic E- and N-cadherin expression was detected by immunoblotting in ethanol-exposed embryos. The ethanol action may be due to the disruption of neuroepithelial and mesodermal cell–cell adhesion leading to upregulation of cadherin expression in cells. Previous work (Radice et al., 1997) reported that in homozygous mutant embryo for N-cadherin, neurulation and somitogenesis initiated apparently normal. However, the resulting structures were malformed, producing small somites with irregular shapes and less cohesive cells and epithelial organization of somites partially disrupted. Since the differentiation and migration of sclerotomal cells coincides with the downregulation of N-cadherin, and that N-and E-cadherin plays a critical role in early normal organ development as morphoregulatory molecules for differentiation, segregation, and migration of embryonic cells, the abnormal spatiotemporal regulation of cadherin expression can be the cause for abnormalities of organogenic exposed embryos. Therefore, it is possible that deregulation or overexpression of N-cadherin plays an important role in abnormalities of NT after ethanol exposure. Similarly, since mice lacking E-cadherin expression in the epidermis die shortly after birth (Tunggal et al., 2005), we suggest that a consequence of altered E-cadherin expression may be the induction of increased risk of organogenic embryo death. In our experimental model, upregulation of E- and N-cadherin expression can be proposed as a mechanism that compensates for the dissociating effects of ethanol on embryonic cell junctions.

In conclusion, we demonstrated that perigestational ethanol consumption by CF-1 mice induces severe damage of embryo development at organogenesis as revealed by delayed differentiation, growth deficiencies, and abnormal morphogenesis of the NT. These ethanol effects may be the induction of cell–cell adhesion disruption leading to abnormal cadherin expression in embryonic cells and suggesting that upregulation of cell adhesion molecules may be a mechanism of reduced embryo viability, delayed differentiation, and NT defects.

ACKNOWLEDGMENTS

The authors thank Hector Chiocchio of the CEFYBO-CONICET for his excellent technical assistance with the scanning microscopy. This work was supported by EC-Grants: Re-Entry Grant PLACIRH (Programa Latinoamericano de Capacitación e Investigación en Reproducción Humana [Latin American Program for Training and Investigation in Human Reproduction], PRE-037/2000), PIP-CONICET: 5917 and 114-200801-00014 from the Consejo Nacional de Investigaciones Científicas y Técnicas (CONICET), Argentina, BID-PICT-2008-2210

from the National Agency (Argentina), and UBACYT 20020090200655 of the University of Buenos Aires, Argentina.

EC-Grants: Re-Entry Grant PLACIRH (Programa Latinoamericano de Capacitación e Investigación en Reproducción Humana [Latin American Program for Training and Investigation in Human Reproduction], PRE-037/2000), PIP-CONICET: 5917 and 114-200801-00014 from the Consejo Nacional de Investigaciones Científicas y Técnicas (CONICET), Argentina, BID-PICT-2008-2210 from the National Agency (Argentina), and UBACYT 20020090200655 of the University of Buenos Aires, Argentina.

REFERENCES

Ahlgren SC, Thakur V, Bronner-Fraser M. 2002. Sonic hedgehog rescues cranial neural crest from cell death induced by ethanol exposure. Proc Natl Acad Sci USA 99:10476–10481.

Allan AM, Chynoweth J, Tyler LA, Caldawell KK. 2003. A mouse model of prenatal ethanol exposure using a voluntary drinking paradigm. Alcohol Clin Exp Res 27:2009–2016.

Allebeck P, Olsen J. 1998. Alcohol and fetal damage. Alcohol Clin Exp Res 22:329S–332S.

Amini SA, Dunkley PR, Murdoch RN. 1996. Teratogenic effects of etanol in the Quackenbush Special mouse. Drug Alcohol Depend 41:61–69.

Aoto K, Nishimura T, Eto K, Motoyama J. 2002. GLI3 regulates Fgf8 expression and apoptosis in the developing neural tube, face, and limb bud. Dev Biol 251:320–332.

Aragón AS, Kalberg WO, Buckley D, et al. 2008. Neuropsychological study of FASD in a sample of American Indian children: processing simple versus complex information. Alcohol Clin Exp Res 32:2136–2148.

BoehmII SL, Moore EM, Walsh CD, et al. 2008–2009. Using drinking in the dark to modle prenatal binge-like exposure to ethanol in C57BL/6J mice. Dev Psychobiol 50:566–578.

Canteros G, Rettori V, Franchi A, et al. 1995. Ethanol inhibits luteinizing hormone-releaseing hormone (LHRH) secretion by blocking the response of LHRH neuronal terminals to nitric oxide. Proc Natl Acad Sci USA 92:3416–3420.

Cebral E, Lasserre A, Faletti AB, Gimeno MAF. 1998a. Response to ovulatory induction following moderate chronic ethanol administration in mice. Med Sci Res 26:29–31.

Cebral E, Lasserre A, Motta A, Gimeno MAF. 1998b. Mouse oocyte quality and prostaglandin synthesis by cumulus oocyte complex after moderate chronic ethanol intake. Prost Leuk Ess Fatty Acids 58:381–387.

Cebral E, Faletti AB, Jawerbaum A, Paz DA. 2007. Periconceptional alcohol consumption-induced changes in embryonic prostaglandin E levels in mouse organogenesis. Modulation by nitric oxide. Prost Leuk Ess Fatty Acids 76:141–151.

Cebral E, Abrevaya XC, Mudry MD. 2011. Male and female reproductive toxicity induced by sub-chronic ethanol exposure in CF-1 mice. Cell Biol Toxicol, DOI: 10.1007/s10565-011-9185-72011.

Ceccanti M, Alessandra Spagnolo P, Tarani L, et al. 2007. Clinical delineation of fetal alcohol spectrum disorders (FASD) in Italian children: comparison and contrast with other racial/ethnic groups and implications for diagnosis and prevention. Neurosci Biobehav Rev 31:270–277.

Checiu M, Sandor S. 1981. The effect of ethanol upon early development in mice and rats. III. In vivo effect of acute ethanol intoxication upon implantation and early postimplantation stages in mice. Morphol Embryol Physiol 27:117–122.

Checiu MC, Sandor S. 1982. The effect of ethanol upon early development in mice and rats. IV. The effect of acute ethanol intoxication on day 4 of pregnancy upon implantation and early postimplantation development in mice. Morphol Embryol 28:127–133.

Cook CS, Nowotny AZ, Sulik KK. 1987. Fetal alcohol syndrome. Eye malformations in a mouse model. Arch Ophthalmol 105:1576–1581.

Crabbe JC, Belknap JK, Buck KJ. 1994. Genetic animal models of alcohol and drug abuse. Science 264:1715–1723.

Cudd TA. 2005. Animal model system for the study of alcohol teratology. Exp Biol Med 230:389–393.

Da Lee R, Rhee GS, An SM, et al. 2004. Differential gene profiles in developing embryo and fetus in utero exposure to ethanol. J Toxicol Environ Health A 67:2073–2084.

Debelak-Kragtorp KA, Armant DR, Smith SM. 2003. Ethanol-induced cephalic apoptosis requires phospholipase C-dependent intracellular calcium signaling. Alcohol Clin Exp Res 27:515–523.

Dunty WC, Chen S, Zucker RM, et al. 2001. Selective vulnerability of embryonic cell populations to ethanol-induced apoptosis: implications for alcohol-related birth defects and neurodevelopmental disorder. Alcohol Clin Exp Res 25:1523–1535.

Dunty WC, Zucker RM, Sulik KK. 2002. Hindbrain and cranial nerve dysmorphogenesis results from acute maternal ethanol administration. Dev Neurosci 24:328–342.

Gao X, Bian W, Yang J, et al. 2001. A role of N-cadherin in neuronal differentiation of embryonic carcinoma P19 cells. Biochem Biophys Res Commun 284:1098–1103.

George-Weinstein M, Gerhart J, Blitz J, et al. 1997. N-cadherin promotes the commitment and differentiation of skeletal muscle precursor cells. Dev Biol 185:14–24.

Goda Y. 2002. Cadherins communicate structural plasticity of presynaptic and postsynaptic terminals. Neuron 35:1–3.

Goodlett CR, Horn KH. 2001. Mechanisms of alcohol-induced damage to the developing nervous system. Alcohol Res Health 25:175–184.

Guerri C. 2002. Mechanisms involved in central nervous system dysfunctions induced by prenatal ethanol exposure. Neurotox Res 4:327–335.

Gumbiner BM. 2000. Regulation of cadherin adhesive activity. J Cell Biol 148:399–403.

Hanningan JH, Armant DR. 2000. Alcohol in pregnancy and neonatal outcome. Semin Neonatal 5:243–254.

Henery CC, Kaufman MH. 1992. Cleavage rate of haploid and diploid parthenogenetic mouse embryos during the preimplantation period. Mol Reprod Dev 31:258–263.

Herniksen TB, Hjollund NH, Jensen TK, et al. 2004. Alcohol consumption at the time of conception and spontaneous abortion. Am J Epidemiol 160:661–667.

Higashiyama D, Saitsu H, Komada M, et al. 2007. Sequential developmental changes in holoprosencephalic mouse embryos exposed to ethanol during gastrulation period. Birth Defects Res A Clin Mol Teratol 79:513–523.

Hoyme HE, May PA, Kalberg WO, et al. 2005. A practical clinical approach to diagnosis of fetal alcohol spectrum disorders: clarification of the 1996 Institute of Medicine criteria. Pediatrics 115:39–47.

Hunter ES, Tugman JA, Sulik KK, Sadler TW. 1994. Effects of short-term exposure to ethanol on mouse embryos in vitro. Toxicol In Vitro 3:413–421.

Kaufman MH. 1997. The teratogenic effects of alcohol following exposure during pregnancy and its influence on the chromosome constitution of pre-ovulatory egg. Alcohol Alcohol 32:113–128.

Kaufman MH, Bain IM. 1984a. Influence of ethanol on chromosome segregation during the first and second meiotic divisions in the mouse egg. J Exp Zool 230:315–320.

Kaufman MH, Bain IM. 1984b. The development potential of ethanol-induced monosomic and trisomic conceptuses in the mouse. J Exp Zool 231:149–155.

Kaufman MH, Bard JBL. 1999. The anatomical basis of mouse development. London: Academic Press. pp. 220–223.

Kesmodel U, Wisborg K, Olsen SF, et al. 2002. Moderate alcohol intake in pregnancy and the risk of spontaneous abortion. Alcohol Alcohol 37:87–92.

Kido R, Sato I, Tsuda S. 2006. Detection on in vivo DNA damage induced by ethanol in multiple organs of pregnant mice using the alkaline single cell gel electrophoresis (Comet) assay. J Vet Med Sci 68:41–47.

Kotch LE, Sulik KK. 1992a. Experimental Fetal Alcohol Syndrome: Proposed pathogenic basis for a variety of associated facial and brain anomalies. Am J Med Genet 44:168–176.

Kotch LE, Sulik KK. 1992b. Patterns of ethanol-induced cell death in the developing nervous system of mice; neural fold states through the time of anterior neural tube closure. Int J Dev Neurosci 10:273–279.

Lamarche F, Gonthier B, Signorini N, et al. 2004. Impact of ethanol and acetaldehyde on DNA and cell viability of cultured neurons. Cell Biol Toxicol 20:361–374.

Lee RD, An SM, Kim SS, et al. 2005. Neurotoxic effects of alcohol and acetaldehyde during embryonic development. J Toxicol Environ Health A 68:2147–2162.

Lemoine P, Harousseau H, Borteyru JP, Menuet JC. 1968. Children of alcoholic parents: Anomalies observed in 127 cases. Quest Medicale 21:476–482.

Lowry OH, Rosebrough NJ, Farr AL, Randall RJ. 1951. Protein measurement with the Folin-phenol reagent. J Biol Chem 193:265–275.

Mancinelli R, Ceccanti M, Laviola G. 2007. Fetal alcohol spectrum disorders (FASD): from experimental biology to the search for treatment. Neurosci Biobehav Rev 31:165–167.

Mattson SN, Riley EP. 2008. A review of the neurobehavioraql deficits in children with fetal alcohol syndrome of prenatal exposure to alcohol. Alcohol Clin Exp Res 22:279–294.

Menegola E, Broccia ML, Di Renzo F, Giavini E. 2001. Acetaldehyde in vitro exposure and apoptosis: a possible mechanism of teratogenesis. Alcohol 23:35–39.

Miller MW. 1986. Effects of alcohol on the generation and migration of cerebral cortical neurons. Science 233:1308–1311.
Miller MW. 2006. Growth factor regulation of cell proliferation is altered by ethanol. In: Miller MW, editor. Brain development. Normal processes and the effects of alcohol and nicotine. New York: Oxford University Press. pp. 182–198.
Miller MW, Nowakowski RS. 1991. Effect of prenatal exposure to ethanol on the cell cycle kinetics and growth fraction in the proliferative zones of fetal rat cerebral cortex. Alcohol Clin Exp Res 15:229–232.
Minana R, Climent E, Barettino D, et al. 2000. Alcohol exposure alters the expression pattern of neural cell adhesion molecules during brain development. J Neurochem 75:954–964.
Montell DJ. 1999. The genetics of cell migration in *Drosophila melanogaster* and *Caenorhabditis elegans* development. Development 126:3035–3046.
Mooney SM, Miller MW. 2007. Time-specific effects of ethanol exposure on cranial nerve nuclei: gastrulation and neurogenesis. Exp Neurol 205:56–63.
Nakatsuji N. 1983. Craniofacial malformation in *Xenopus laevis* tadpoles caused by the exposure of early embryos to ethanol. Teratology 28:299–305.
Nelson WJ. 2003. Adaptation of core mechanisms to generate cell polarity. Nature 422:766–774.
Nose A, Nagafuchi A, Takeichi M. 1988. Expressed recombinant cadherins mediate cell sorting in models systems. Cell 54:993–1001.
Parnell SE, Dehart DB, Wills TA, et al. 2006. Maternal oral intake mouse model for fetal alcohol spectrum disorders: ocular defects as a measure of effect. Alcohol Clin Exp Res 30:1791–1798.
Peng Y, Yang PH, Ng SS, et al. 2004. A critical role of Pax6 in alcohol-induced fetal microcephaly. Neurobiol Dis 16:370–376.
Radice GL, Rayburn H, Matsunami H, et al. 1997. Developmental defects in mouse embryos lacking N-cadherin. Dev Biol 181:64–78.
Rhodes JS, Ford MM, Yu C-H, et al. 2007. Mouse inbred strain differences in ethanol drinking to intoxication. Genes Brain Behav 6:1–18.
Sakamoto A, Murata K, Susuki H, et al. 2008. Immunohistochemical observation of co-expression of E-and N-cadherin in rat organogenesis. Acta Histochem Cytochem 41:143–147.
Sampson PD, Streissguth AP, Bookstein FL, Barr HM. 2000. On categorization in analyses of alcohol teratogenesis. Environ Health Perspect 3:421–428.
Sanchis R, Esquifino A, Guerri C. 1985. Chronic ethanol intake modifies estrous cyclicity and alters prolactin and LH levels. Pharmacol Biol Behav 23:221–224.
Savagner P. 2001. Leaving the neighborhood: molecular mechanisms involved during epithelial-mesenchymal transition. BioEssays 23:912–923.
Simpson ME, Duggal S, Keiver K. 2005. Prenatal ethanol exposure has differential effects on fetal growth and skeletal ossification. Bone 36:521–532.
Soltes BA, Anderson R, Radwanska E. 1996. Morphologic changes in offspring of female mice exposed to ethanol before conception. Am J Obstet Gynecol 175:1158–1162.
Sulik KK, Lauder JM, Dehart DB. 1984. Brain malformations in prenatal mice following acute maternal ethanol administration. Int J Dev Neurosci 2:203–214.
Susuki A, Susuki R, Furuno T, et al. 2004. N-cadherin plays a role in the synapse-like structures between mast cells and neuritis. Biol Pharm Bull 27:1891–1894.
Takeichi M. 1990. Cadherins: a molecular family important in selective cell-cell adhesion. Annu Rev Biochem 59:237–252.
Takeichi M. 1991. Cadherin cell adhesion receptors as a morphogenetic regulator. Science 251:1451–1455.
Tepass U, Truong K, Godt D, et al. 2000. Cadherins in embryonic and neural morphogenesis. Nat Rev Mol Cell Biol 1:91–100.
Tunggal JA, Helfrich I, Schmitz A, et al. 2005. E-cadherin is essential for in vivo epidermal barrier function by regulating tight junctions. The EMBO Journal 24:1146–1156.
Wheelock MJ, Shintani Y, Maeda M, et al. 2008. Cadherin switching. J Cell Sci 121:727–735.
Wiebold JL, Becker WC. 1987. In vivo and in vitro effects of ethanol on mouse preimplantation embryos. J Reprod Fertil 80:49–57.
Xu X, Li WEI, Huang GY, et al. 2001. Modulation of mouse neural crest cell motility by N-cadherin and connexin 43 gap junctions. J Cell Biol 154:217–229.